ANDES, the high resolution spectrograph for the ELT: science goals, project overview and future developments

A. Marconi[1,2], M. Abreu[3], V. Adibekyan[4,5], V. Alberti[6], S. Albrecht[7], J. Alcaniz[8], M. Aliverti[9], C. Allende Prieto[10,11], J. D. Alvarado Gómez[12], C. S. Alves[13,14], P. J. Amado[15], M. Amate[10], M. I. Andersen[16,17], S. Antoniucci[18], E. Artigau[19,20], C. Bailet[21], C. Baker[22], V. Baldini[6], A. Balestra[23], S. A. Barnes[12,24], F. Baron[19,20,25], S. C. C. Barros[4,5], S. M. Bauer[12], M. Beaulieu[21], O. Bellido-Tirado[12], B. Benneke[19,20], T. Bensby[26], E. A. Bergin[27], P. Berio[21], K. Biazzo[18], L. Bigot[21], A. Bik[28], J. L. Birkby[29], N. Blind[30], O. Boebion[21], I. Boisse[31,32], E. Bolmont[30,33], J. S. Bolton[34], M. Bonaglia[2], X. Bonfils[35], L. Bonhomme[36], F. Borsa[9], J.-C. Bouret[31], A. Brandeker[28], W. Brandner[37], C. H. Broeg[38,39], M. Brogi[40,41,42], D. Brousseau[43], A. Brucalassi[2], J. Brynnel[12], L. A. Buchhave[44], D. F. Buscher[22], L. Cabona[9], A. Cabral[3], G. Calderone[6], R. Calvo-Ortega[15], F. Cantalloube[45], B. L. Canto Martins[46], L. Carbonaro[2], Y. Caujolle[21], G. Chauvin[21], B. Chazelas[30], A.-L. Cheffot[2], Y. S. Cheng[47], A. Chiavassa[21], L. Christensen[48,16], R. Cirami[6], M. Cirasuolo[49], N. J. Cook[19,20], R. J. Cooke[50], I. Coretti[6], S. Covino[9], N. Cowan[51], G. Cresci[2], S. Cristiani[6,52,53], V. Cunha Parro[54], G. Cupani[6,53], V. D'Odorico[6,55,53], K. Dadi[47], I. de Castro Leão[46], A. De Cia[49], J. R. De Medeiros[46], F. Debras[36], M. Debus[56], A. Delorme[49], O. Demangeon[4,5], F. Derie[49], M. Dessauges-Zavadsky[30], P. Di Marcantonio[6], S. Di Stefano[57,6], F. Dionies[12], A. Domiciano de Souza[21], R. Doyon[19,20,25], J. Dunn[58], S. Egner[49], D. Ehrenreich[30,33], J. P. Faria[30], D. Ferruzzi [2], C. Feruglio[6], M. Fisher[22], A. Fontana[18], B. S. Frank[59,60], C. Fuesslein[12], M. Fumagalli[61,6], T. Fusco[62,31], J. Fynbo[16,17], O. Gabella[63], W. Gaessler[37], E. Gallo[27], X. Gao[59], L. Genolet[30], M. Genoni[9], P. Giacobbe[41], E. Giro[23,64], R. S. Gonçalves[65,8], O. A. Gonzalez[59], J. I. González Hernández[10,11], C. Gouvret[21], F. Gracia Témich[10], M.G. Haehnelt[66], C. Haniff[22], A. Hatzes[67], R. Helled[68], H.J. Hoeijmakers[26], I. Hughes[69], P. Huke[70,56], Y. Ivanisenko[69], A. S. Järvinen[12], S. P. Järvinen[12], A. Kaminski[71], J. Kern[12], J. Knoche[72], A. Kordt[73,74], H. Korhonen[37], A. J. Korn[74], D. Kouach[75], G. Kowzan[76], L. Kreidberg[37], M. Landoni[9], A. A. Lanotte[69], A. Lavail[75], B. Lavie[30], D. Lee[59], M. Lehmitz[37], J. Li[77], W. Li[22], J. Liske[72], C. Lovis[30], S. Lucatello[23], D. Lunney[59], M. J. MacIntosh[59], N. Madhusudhan[78], L. Magrini[2], R. Maiolino[22,66,79], J. Maldonado[80], L. Malo[19], A. W. S. Man[81], T. Marquart[74], C. M. J. Marques[13,4,82], E. L. Marques[54], P. Martinez[21], A. Martins[4,13], C. J. A. P. Martins[83], J. H. C. Martins[4], P. Maslowski[76], C. A. Mason[48,16], E. Mason[6], R. A. McCracken[47], M.A.F. Melo e Sousa[13,82], P. Mergo[84], G. Micela[80], D. Milaković[53,6], P. Mollière[37], M. A. Monteiro[4], D. Montgomery[59], C. Mordasini[39,38], J. Morin[63], A. Mucciarelli[85,86], M. T. Murphy[87], M. N'Diaye[21], N. Nardetto[21], B. Neichel[31], N. Neri[6], A.T. Niedzielski[88], E. Niemczura[89], B. Nisini[18], L. Nortmann[56], P. Noterdaeme[90,91], N. J. Nunes[3], L. Oggioni[9], F. Olchewsky[36], E. Oliva[2], H. Önel[12], L. Origlia[86], G. Östlin[28], N. N.-Q. Ouellette[19,20,25], E. Palle[10,11], P. Papaderos[4,3], G. Pariani[9], L. Pasquini[49], J. Peñate Castro[10], F. Pepe[30], C. Peroux[49], L. Perreault Levasseur[19,92], S. Perruchot[32], P. Petit[36], O. Pfuhl[49], L. Pino[2], J. Piqueras[93], N. Piskunov[74], A. Pollo[94,95], K. Poppenhaeger[12,96], M. Porru[6], J. Puschnig[74], A. Quirrenbach[71], E. Rauscher[27], R. Rebolo[10,97,11], E. M. A. Redaelli[9], S. Reffert[71], D. T. Reid[47], A. Reiners[56], P. Richter[96,12], M. Riva[9], S. Rivoire[63], C. Rodríguez-López[15], I. U. Roederer[27,98,99], D. Romano[86], M. Roth[67], S. Rousseau[21], J. Rowe[100], A. Saccardi[101], S. Salvadori[1,2], N. Sanna[2], N. C. Santos[4,5], P. Santos Diaz[30], J. Sanz-Forcada[93], M. Sarajlic[39], J.-F. Sauvage[62,31], D. Savio[2,1], A Scaudo[9], S. Schäfer[56], R. P. Schiavon[102], T. M. Schmidt[30], C. Selmi[2], R. Simoes[10], A. Simonnin[21], S. Sivanandam[103,104], M. Sordet[30], R. Sordo[23], F. Sortino[9],

Ground-based and Airborne Instrumentation for Astronomy X, edited by Julia J. Bryant, Kentaro Motohara, Joël R. D. Vernet, Proc. of SPIE Vol. 13096, 1309613
© 2024 SPIE · 0277-786X · doi: 10.1117/12.3017966

D. Sosnowska[30], S. G. Sousa[4], A. Spang[21], R. Spiga[2], E. Stempels[74], J. R. Y. Stevenson[59], K. G. Strassmeier[12,96], A. Suárez Mascareño[10,11], A. Sulich[6], X. Sun[22], N. R. Tanvir[105], F. Tenegi-Sanginés[10], S. Thibault[43], S. J. Thompson[22], P. Tisserand[106], A. Tozzi[2], M. Turbet[107,108], J.-P. Véran[58], P. Vallée[19,20,25], I. Vanni[1,2], R. Varas[15], A. Vega-Moreno[10], K. A. Venn[109], A. Verma[110], J. Vernet[49], M. Viel[111,53,6], G. Wade[112], C. Waring[59], M. Weber[12], J. Weder[39], B. Wehbe[3], J. Weingrill[12], M. Woche[12], M. Xompero[2], E. Zackrisson[74], A. Zanutta[9], M. R. Zapatero Osorio[93], M. Zechmeister[56], and J. Zimara[56]

[1]Department of Physics and Astronomy, University of Florence, Italy

[2]INAF - Osservatorio Astrofisico di Arcetri, Largo E. Fermi 5, I-50125 Firenze, Italy

[3]Instituto de Astrofísica e Ciências do Espaço, Universidade de Lisboa, Faculdade de Ciências, Campo Grande, PT1749-016 Lisboa, Portugal

[4]Instituto de Astrofísica e Ciências do Espaço, Universidade do Porto, CAUP, Rua das Estrelas, PT4150-762 Porto, Portugal

[5]Departamento de Física e Astronomia, Faculdade de Ciências, Universidade do Porto, Rua do Campo Alegre, 4169-007 Porto, Portugal

[6]INAF - Osservatorio Astronomico di Trieste, via G. B. Tiepolo 11, 34143 Trieste, Italy

[7]Stellar Astrophysics Centre, Department of Physics and Astronomy, Aarhus University, Ny Munkegade 120, 8000 Aarhus C, Denmark

[8]Departamento de Astronomia, Observatório Nacional, 20921-400, Rio de Janeiro, RJ, Brazil

[9]INAF - Osservatorio Astronomico di Brera, Via E. Bianchi 46, 23807 Merate (LC), Italy

[10]Instituto de Astrofísica de Canarias (IAC), E-38200 La Laguna, Tenerife, Spain

[11]Universidad de La Laguna, Dept. Astrofísica, E-38206 La Laguna, Tenerife, Spain

[12]Leibniz Institute for Astrophysics Potsdam (AIP), An der Sternwarte 16, D-14482 Potsdam, Germany

[13]Centro de Astrofísica da Universidade do Porto, Rua das Estrelas, PT4150-762 Porto, Portugal

[14]Department of Physics and Astronomy, University College London, Gower Street, London WC1E 6BT, United Kingdom

[15]Instituto de Astrofísica de Andalucía, CSIC, Glorieta de la Astronomía s/n, 18008 Granada, Spain

[16]Niels Bohr Institute, University of Copenhagen, Jagtvej 128, DK-2200, Copenhagen N, Denmark

[17]Cosmic Dawn Center (DAWN)

[18]INAF - Osservatorio Astronomico di Roma, via Frascati 33, I-00078 Monte Porzio Catone (RM), Italy

[19]Département de Physique, Université de Montréal, 1375 Avenue Thérèse-Lavoie-Roux, Montréal, QC, H2V 0B3, Canada

[20]Institut Trottier de recherche sur les exoplanètes, Université de Montreal, Canada

[21]Université Côte d'Azur, Observatoire de la Côte d'Azur, CNRS, Lagrange, CS 34229, Nice, France

[22]Cavendish Laboratory, University of Cambridge, J J Thomson Avenue, Cambridge, CB3 0HE, UK

[23]INAF - Osservatorio Astronomico di Padova, Vicolo dell'Osservatorio, 5, 35122 Padova, Italy

[24]Space Science Institute, USA

[25]Observatoire du Mont-Mégantic, Université de Montreal, Canada
[26]Division of Astrophysics, Department of Physics, Lund University, Box 118, 22100 Lund, Sweden
[27]Department of Astronomy, University of Michigan, 311 West Hall, 1085 S. University Ave., Ann Arbor, MI, 48109, USA
[28]The Oskar Klein Center, Department of Astronomy, Stockholm University, AlbaNova 10691, Stockholm, Sweden
[29]Astrophysics, Department of Physics, University of Oxford, Denys Wilkinson Building, Keble Road, Oxford, OX1 3RH, UK
[30]Observatoire Astronomique de l'Université de Genève, Chemin Pegasi 51, Versoix, CH-1290, Switzerland
[31]Aix Marseille Univ, CNRS, CNES, LAM, Marseille, France
[32]Observatoire de Haute-Provence, CNRS, Université d'Aix-Marseille, 04870 Saint-Michel-l'Observatoire, France
[33]Centre Vie dans l'Univers, Faculté des sciences, Université de Genève, quai Ernest-Ansermet 30, 1211 Genève 4, Switzerland
[34]School of Physics and Astronomy, University of Nottingham, University Park, Nottingham, NG7 2RD, UK
[35]Université Grenoble Alpes, CNRS, IPAG, F-38000 Grenoble, France
[36]IRAP, Université de Toulouse, UMR CNRS F-5277, UPS, Toulouse, France
[37]Max-Planck-Institut für Astronomie, Königstuhl 17, D-69117 Heidelberg, Germany
[38]Center for Space and Habitability, Gesellsschaftstrasse 6, 3012 Bern, Switzerland
[39]Physikalisches Institut, University of Bern, Sidlerstrasse 5, 3012 Bern, Switzerland
[40]Department of Physics, University of Warwick, Coventry CV4 7AL, UK
[41]INAF - Osservatorio Astrofisico di Torino, Via Osservatorio 20, I-10025, Pino Torinese, Italy
[42]Centre for Exoplanets and Habitability, University of Warwick, Gibbet Hill Road, Coventry CV4 7AL, UK
[43]Université Laval, Quebec, Canada
[44]DTU Space, National Space Institute, Technical University of Denmark, Elektrovej 328, DK-2800 Kgs. Lyngby, Denmark
[45]Univ. Grenoble Alpes, CNRS, IPAG, 38000 Grenoble, France
[46]Departamento de Física Teórica e Experimental, Universidade Federal do Rio Grande do Norte, Campus Universitário, Natal, RN, 59072-970, Brazil
[47]Scottish Universities Physics Alliance (SUPA), Institute of Photonics and Quantum Sciences, School of Engineering and Physical Sciences, Heriot-Watt University, Edinburgh EH14 4AS, UK
[48]Cosmic Dawn Center (DAWN), Copenhagen, Denmark
[49]European Southern Observatory, Karl-Schwarzschild-Str 2, D-86748 Garching b. München, Germany
[50]Centre for Extragalactic Astronomy, Durham University, South Road, Durham DH1 3LE, UK
[51]McGill University, Canada
[52]INFN - Sezione di Trieste, Italy
[53]IFPU - Institute for Fundamental Physics of the Universe, via Beirut 2, I-34151 Trieste, Italy
[54]Instituto Mauá de Tecnologia, Brazil

[55]Scuola Normale Superiore Piazza dei Cavalieri 7, I-56126 Pisa, Italy
[56]Institut für Astrophysik und Geophysik, Georg-August-Universität, Friedrich-Hund-Platz 1, 37077 Göttingen, Germany
[57]Department of Physics, University of Trieste, Italy
[58]NRC Herzberg Astronomy and Astrophysics Research Centre, Canada
[59]UK Astronomy Technology Centre, Royal Observatory, Blackford Hill, Edinburgh, EH9 3HJ, Scotland, UK
[60]Department of Astronomy, University of Cape Town, Private Bag X3, Rondebosch 7701, South Africa
[61]Dipartimento di Fisica "G. Occhialini", Università degli Studi di Milano Bicocca, Piazza della Scienza 3, 20126 Milano, Italy
[62]DOTA, ONERA, F-13661 Salon cedex Air, France
[63]Laboratoire Univers et Particules de Montpellier, Université de Montpellier, CNRS, France
[64]INFN - Sezione di Padova, Italy
[65]Departamento de Física, Universidade Federal Rural do Rio de Janeiro, Seropédica, Rio de Janeiro, 23897-000, Brazil
[66]Kavli Institute for Cosmology and Institute of Astronomy, University of Cambridge, UK
[67]Thueringer Landessternwarte Tautenburg, Sternwarte 5, D-07778 Tautenburg, Germany
[68]Institute for Computational Science, Center for Theoretical Astrophysics & Cosmology, University of Zurich, Winterthurerstr. 190, CH-8057 Zurich, Switzerland
[69]Département d'Astronomie, Université de Genève, Chemin Pegasi 51, CH-1290 Versoix, Switzerland
[70]Institute for Laser and Optics, Hochschule Emden/Leer, Germany
[71]Landessternwarte, Zentrum für Astronomie der Universität Heidelberg, Königstuhl 12, 69117 Heidelberg, Germany
[72]Hamburger Sternwarte, Universität Hamburg, Gojenbergsweg 112, 21029 Hamburg, Germany
[73]Institut für Theoretische Astrophysik, Zentrum für Astronomie der Universität Heidelberg, Albert-Ueberle-Str 2, 69120 Heidelberg
[74]Division of Astronomy and Space Physics, Department of Physics and Astronomy, Uppsala University, Box 516, 75120 Uppsala, Sweden
[75]Observatoire Midi-Pyrénées, CNRS, Université Paul Sabatier, 14 Av. Ed. Belin 31400 Toulouse, France
[76]Institute of Physics, Faculty of Physics, Astronomy and Informatics, Nicolaus Copernicus University in Toruń, ul. Grudziądzka 5, 87-100 Toruń, Poland
[77]Purple Mountain Observatory, Chinese Academy of Sciences, 10 Yuanhua Road, Nanjing 210023, China
[78]Institute of Astronomy, Madingley Road, University of Cambridge, Cambridge CB3 0HA, UK
[79]Department of Physics and Astronomy, University College London, UK
[80]INAF - Osservatorio Astronomico di Palermo, Italy
[81]The University of British Columbia, Canada
[82]Faculdade de Ciências, Universidade do Porto, Rua do Campo Alegre, 4150-007 Porto, Portugal
[83]Department of Electrical Engineering, Federal University of Rio Grande do Norte, Brazil
[84]Laboratory of Optical Fibers Technology, Institute of Chemical Sciences, Faculty of Chemistry, Maria Curie Sklodowska University, Sklodowska Sq 3, 20-031 Lublin, Poland

[85]Department of Physics and Astronomy, University of Bologna, Italy
[86]INAF - Osservatorio di Astrofisica e Scienza dello Spazio di Bologna, Italy
[87]Centre for Astrophysics and Supercomputing, Swinburne University of Technology, Hawthorn, Victoria 3122, Australia
[88]Institute of Astronomy, Faculty of Physics, Astronomy and Informatics, Nicolaus Copernicus University in Toruń, ul. Grudziądzka 5, 87-100 Toruń, Poland
[89]University of Wroclaw, Astronomical Institute, Kopernika 11, 51-622 Wroclaw, Poland
[90]Institut d'Astrophysique de Paris, UMR 7095, CNRS and SU, 98bis bd Arago, 75014 Paris, France
[91]Franco-Chilean Laboratory for Astronomy, IRL 3386, CNRS and U. de Chile, Casilla 36-D, Santiago, Chile
[92]Quebec Artificial Intelligence Institute (Mila), 6666, rue St-Urbain #200, Montréal, Québec, H2S 3H1 CA
[93]Centro de Astrobiología (CAB, CSIC-INTA), Carretera de Ajalvir km 4, E-28850 Torrejón de Ardoz, Madrid, Spain
[94]Astronomical Observatory of the Jagiellonian University; ul. Orla 171, 30-244 Cracow, Poland
[95]National Centre for Nuclear Research, Pasteura 7, 02-093 Warsaw, Poland
[96]Potsdam University, Institute for Physics and Astronomy, Karl-Liebknecht-Straße 24/25, 14476 Potsdam, Germany
[97]Consejo Superior de Investigaciones Científicas (CSIC), Spain
[98]Department of Physics, North Carolina State University, 2401 Stinson Dr, Box 8202, Raleigh, NC 27695, USA
[99]Joint Institute for Nuclear Astrophysics - Chemical Evolution of the Elements, USA
[100]Bishop's University, Canada
[101]GEPI, Observatoire de Paris, Université PSL, CNRS, 5 Place Jules Janssen, 92190 Meudon, France
[102]Astrophysics Research Institute, Liverpool John Moores University, 146 Brownlow Hill, Liverpool, L3 5RF, UK
[103]Dunlap Institute for Astronomy & Astrophysics, University of Toronto, 50 St. George St., Toronto, Ontario, M5S 3H4, Canada
[104]Department of Astronomy & Astrophysics, University of Toronto, 50 St. George St., Toronto, Ontario, Canada M5S 3H4
[105]School of Physics and Astronomy, University of Leicester, University Road, Leicester, LE1 7RH, UK
[106]Sorbonne Université, CNRS, UMR 7095, Institut d'Astrophysique de Paris, 98 bis bd Arago, 75014 Paris, France
[107]Laboratoire de Météorologie Dynamique/IPSL, CNRS, Sorbonne Université, École Normale Supérieure, PSL Research University, École Polytechnique, 75005 Paris, France
[108]Laboratoire d'astrophysique de Bordeaux, Univ. Bordeaux, CNRS, B18N, allée Geoffroy Saint-Hilaire, 33615 Pessac, France
[109]University of Victoria, Department of Physics & Astronomy, Elliott Building, Room 101, 3800 Finnerty Road, Victoria, BC, V8P 5C2, Canada
[110]Sub-department of Astrophysics, Denys Wilkinson Building, University of Oxford, Keble Road, Oxford, OX1 3RH, UK

[111]SISSA - International School for Advanced Studies, Via Bonomea 265, 34136 Trieste, Italy
[112]Department of Physics and Space Science, Royal Military College of Canada, Kingston, Ontario, K7K7B4, Canada

ABSTRACT

The first generation of ELT instruments includes an optical-infrared high resolution spectrograph, indicated as ELT-HIRES and recently christened ANDES (ArmazoNes high Dispersion Echelle Spectrograph). ANDES consists of three fibre-fed spectrographs ([U]BV, RIZ, YJH) providing a spectral resolution of ∼100,000 with a minimum simultaneous wavelength coverage of 0.4-1.8 μm with the goal of extending it to 0.35-2.4 μm with the addition of an U arm to the BV spectrograph and a separate K band spectrograph. It operates both in seeing- and diffraction-limited conditions and the fibre-feeding allows several, interchangeable observing modes including a single conjugated adaptive optics module and a small diffraction-limited integral field unit in the NIR. Modularity and fibre-feeding allows ANDES to be placed partly on the ELT Nasmyth platform and partly in the Coudé room. ANDES has a wide range of groundbreaking science cases spanning nearly all areas of research in astrophysics and even fundamental physics. Among the top science cases there are the detection of biosignatures from exoplanet atmospheres, finding the fingerprints of the first generation of stars, tests on the stability of Nature's fundamental couplings, and the direct detection of the cosmic acceleration. The ANDES project is carried forward by a large international consortium, composed of 35 Institutes from 13 countries, forming a team of almost 300 scientists and engineers which include the majority of the scientific and technical expertise in the field that can be found in ESO member states.

Keywords: ground-based instruments, high resolution spectrographs, infrared spectrographs, extremely large telescopes, exoplanets, stars and planets formation, physics and evolution of stars, physics and evolution of galaxies, cosmology, fundamental physics

1. INTRODUCTION

At first light in 2028, the European Extremely Large Telescope (ELT) will be the largest ground-based telescope at visible and infrared wavelengths. The flagship science cases supporting the successful ELT construction proposal were the detection of life signatures in Earth-like exoplanets and the direct detection of the cosmic expansion re-acceleration. It is no coincidence that both science cases require observations with a high-resolution spectrograph. Over the past few decades high-resolution spectroscopy has been a truly interdisciplinary tool, which has enabled some of the most extraordinary discoveries spanning all fields of Astrophysics, from Exoplanets to Cosmology. Astronomical high-resolution spectrometers have allowed scientists to go beyond the classical domain of astrophysics and to address some of the fundamental questions of Physics. In the wide-ranging areas of research exploiting high-resolution spectroscopy, European scientists have been extremely successful, thanks to the exquisite suite of medium/high-resolution spectrographs that ESO provides to its community. UVES, FLAMES, CRIRES, X-Shooter and HARPS have enabled European teams to lead in many areas of research. ESPRESSO, which has recently joined this suite of very successful instruments, is fulfilling its promise of truly revolutionizing some of these research areas. The scientific interest and high productivity in this field of research is reflected by the fact that more than 30% of ESO publications can be attributed to medium/high-resolution spectrographs. However, it is becoming increasingly clear that, in most areas of research, high-resolution spectroscopy has reached or is approaching the *photon-starved* regime at 8-10m class telescopes. Despite major progress on the instrumentation front, further major advances in these fields desperately require the collecting area of Extremely Large Telescopes. When defining the ELT instrumentation, ESO commissioned two phase-A studies for high-resolution spectrographs, CODEX (Pasquini et al.,[1] covering the 370 nm – 710 nm wavelengths range) and SIMPLE (Origlia et al.,[2] covering the 840 nm – 2400 nm wavelengths range), which were started in 2007 and completed in 2010. These studies demonstrated the importance of optical and near-IR high-resolution spectroscopy at the ELT and ESO thus decided to include a High-REsolution Spectrograph (HIRES) in the ELT instrumentation roadmap. Soon after conclusion of the respective phase A studies the CODEX

Send correspondence to A. Marconi (alessandro.marconi@inaf.it)

and SIMPLE consortia realized the great scientific importance of covering the optical and near-infrared spectral ranges simultaneously. This marked the birth of the HIRES initiative (hires-eelt.org) that started developing the concept of an X-Shooter-like spectrograph, but with high resolution, capable of providing R∼100.000 over the full UV, optical and near infrared wavelength ranges. Following a community workshop in September 2012 the HIRES Initiative prepared a White Paper summarizing a wide range of science cases proposed by the community (Maiolino et al.[3]), and a Blue Book with a preliminary technical instrument concept (Riva et al. 2015).

With the start of construction of the ELT, the HIRES Initiative has decided to organize itself as the HIRES Consortium and has recruited additional institutes, which expressed their interest in HIRES. The consortium, strongly motivated by the unprecedented scientific achievements that the combination of such an instrument with the ELT will enable, was commissioned to perform a Phase A study by ESO which was successfully carried out in 2016-2018. The Consortium was then involved in several pre-Phase B activities in preparation of the start of construction until the ESO Council approved the Construction of HIRES in December 2021. The instrument was then renamed ANDES (ArmazoNes high Dispersion Echelle Spectrograph, andes.inaf.it) and the ANDES Consortium started to formally organize with the signature of the ANDES Consortium agreement where 25 Partners represent 33 institutes from ESO Member States, Brazil, Canada and USA. ANDES started Phase B activities in September 2022: this Phase B1 was successfully concluded in October 2023 with the System Architecture Review (SAR). The construction has finally formally started in June 2024, with the signature of the Construction Agreement with ESO. The conclusion of Phase B and the beginning of subsequent phases is planned in mid-2025, with the aim of bringing ANDES to the telescope in late 2031/early 2032.

This paper provides a general description of the ANDES project, science and consortium. In section 2 we describe the ANDES science goals and priorities, in section 3 the instrument concept, in section 4 the consortium and its organization, and in Section 5 cost estimates and schedule.

2. SCIENCE GOALS

2.1 Exoplanets and Protoplanetary Disks

Characterization of exoplanets atmospheric composition and the exploration of habitable zone planets. The study of exoplanet atmospheres is essential for understanding the diversity, formation, and potential habitability of planetary systems. Atmospheric analysis can reveal a planet's composition, structure, and climate, providing insights into its origins and evolutionary history. Specifically, the detection of atmospheric gases such as oxygen, methane, and water vapor can indicate biological activity, making these studies crucial in the search for extraterrestrial life. Current techniques for studying exoplanet atmospheres include transmission and emission spectroscopy. During a transit, starlight passes through the planet's atmosphere, allowing for the detection of specific molecular signatures in the transmission spectrum. Emission spectroscopy measures the thermal emission from a planet, offering details about its atmospheric composition and temperature. The combination of ELT and ANDES promises to significantly advance the field of exoplanet atmospheric research allowing to pursue ambitious scientific objectives like the characterization of exoplanets atmospheric composition and the exploration of habitable zone planets.

Understanding the chemical composition of exoplanet atmospheres is crucial for identifying potentially habitable planets. ANDES's high spectral resolution (R $\simeq$ 100,000) will enable the detection of faint spectral lines, in between telluric absorption lines, facilitating the identification of trace gases and isotopic ratios. This enhanced sensitivity is essential for detecting biomarkers such as oxygen and methane, which are indicative of biological processes. A comprehensive wavelength coverage (0.5-1.8 μm, with a goal to extend to 0.38-2.4 μm) is also vital for a full characterization of exoplanet atmospheres: ANDES will observe key molecular bands, including those of H_2O, O_2, CO_2, CH_4, NH_3, and other species. This broad coverage ensures that all significant atmospheric components can be detected and analyzed, providing a complete picture of atmospheric composition. Detailed atmospheric dynamics, such as weather patterns and wind speeds, is essential for characterizing exoplanet climates. ANDES's high spectral resolution will allow for precise measurements of Doppler shifts in spectral lines, providing detailed information on atmospheric circulation and dynamics.

While exoplanets atmospheres can be studied with transmission spectroscopy, high-contrast observations can provide direct imaging of exoplanets, allowing to minimize contamination from stellar light. ANDES's ability to

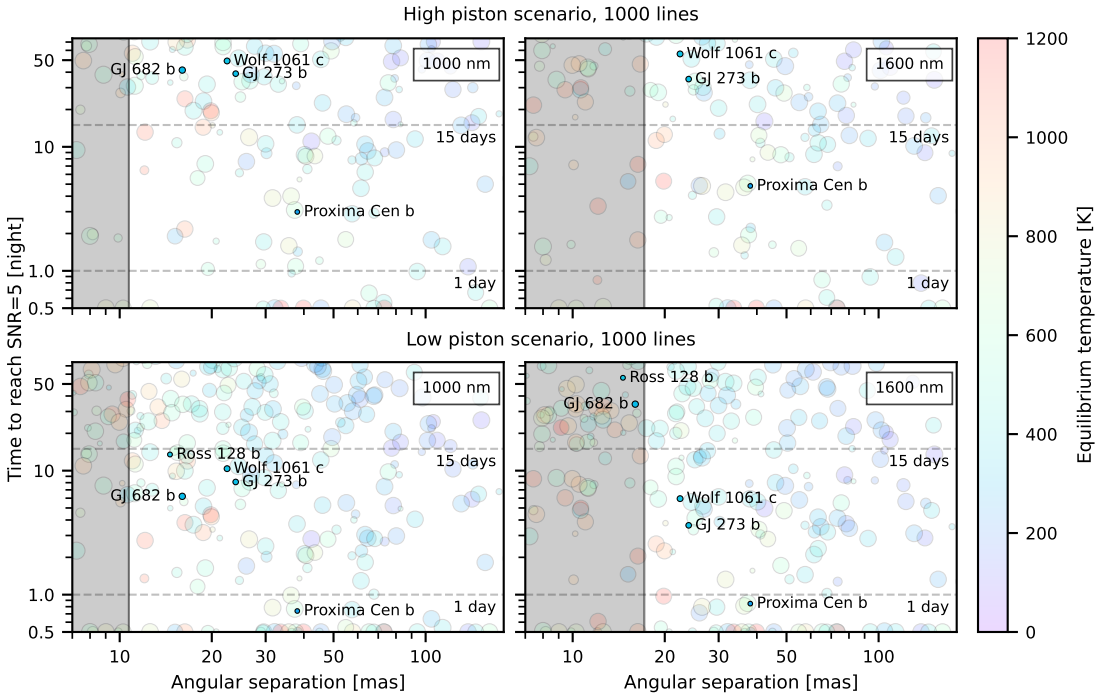

Figure 1. Angular separation between the star and the planet as a function of the exposure time (in nights) necessary to reach a SNR=5 for the known population of planets accessible for atmospheric characterization through reflected light detection at 2 selected wavelengths, we assumed a low piston scenario for the AO correction, and a cross correlation over 1000 absorption lines in the planetary atmosphere. The grey area represents angular separations smaller than twice the ratio between wavelength and telescope diameter. Adapted from Palle et al.[4]

achieve high-contrast observations will enable direct imaging of exoplanets, particularly those that do not transit their host stars. This capability is essential for studying reflected light from exoplanets and for investigating planets in wider orbits that are not accessible through transit spectroscopy.

One of the primary scientific goals of ANDES is to characterize the atmospheres of small, rocky exoplanets in the habitable zone. These planets are of particular interest because they may have conditions suitable for liquid water and, potentially, life. Detailed studies of systems like Proxima Cen and TRAPPIST-1, which contains several Earth-sized planets in the habitable zone, will provide valuable information on the atmospheric conditions of potentially habitable worlds. For instance, a putative CO_2-dominated atmosphere on TRAPPIST-1b planet can be detected and studied at $> 12\sigma$ in 10 transits with transmission spectroscopy (the effects of stellar contamination can be disentangled at high spectral resolution), while Proxima Cen b can be detected at $> 5\sigma$ in 7 h with direct imaging in reflection. The detection of O_2 and H_2O in Proxima Cen b at $> 5\sigma$ will require instead 60 and 4 nights respectively, but these numbers can vary widely depending on the bulk composition of the atmosphere. Figure 1 presents the currently known population of exoplanets accessible for atmospheric characterization through AO-assisted reflected light detection at different wavelengths while Table 1 shows the Golden Sample of planets for ANDES, i.e., the currently known five rocky exoplanets orbiting in the habitable zone of their host stars most favorable for ANDES atmospheric characterization.

Finally, ANDES will work in conjunction with other major observatories, such as NASA-ESA's JWST and ESA's ARIEL mission. Combining high-resolution ground-based data from ANDES with space-based observations will enhance the overall scientific output. This synergy is particularly important for cross-verifying results and obtaining a more comprehensive understanding of exoplanet atmospheres across different spectral ranges.

Protoplanetary disks and the formation and evolution of planetary systems. Understanding the

Name	SpecTyp ($T_{\rm eff}$) [K]	d [pc]	V [mag]	P [d]	$m \sin i$ [$m_\oplus$]	$R_{\rm p}$ [$R_\oplus$]	$T_{\rm eq}$ [K]	sep [mas]	contrast [10^{-8}]	nights
Proxima Cen b	M (2900 K)	1.30	11.01	11.19	1.1	1.07	217	37.3	11.2	0.67
Ross 128 b	M (3163 K)	3.37	11.12	9.87	1.4	1.15	283	14.7	12.5	13
GJ 273 b	M (3382 K)	3.80	9.84	18.65	2.9	1.64	266	24.0	7.52	6.5
Wolf 1061 c	M (3309 K)	4.31	10.10	17.87	3.4	1.81	275	20.7	9.57	5.8
GJ 682 b	M (3237 K)	5.01	10.94	17.48	4.4	2.11	259	16.0	16.0	7.2

Table 1. The Golden Sample planets for ANDES, i.e., the currently known five rocky planets orbiting in the habitable zone of their host stars most favorable for ANDES atmospheric chracterization. Along with several planets properties, we tabulate the number of nights necessary for detecting each planet's atmosphere.

formation and evolution of planetary systems necessitates a detailed study of protoplanetary disks. These disks are the birthplaces of planets, containing the gas and dust from which planetary bodies coalesce. Investigating the composition and distribution of gas within these disks, particularly in the inner regions (within 20 astronomical units), is crucial for comprehending the processes that lead to planet formation and migration.

Protoplanetary disks are best studied through high-resolution spectroscopy, which allows for the separation and analysis of different gas components and mechanisms at play. ANDES, coupled with the large collecting area of the ELT, and with its high spectral resolution and spatial capabilities, will be instrumental in characterizing the gas properties in these regions. Key scientific objectives include the characterization of inner disk gas, the study of disk evolution and the investigation of disk winds and gas dispersal.

By studying forbidden lines of atomic and weakly ionized species at low radial velocities, ANDES will trace the gas in the inner disk regions. This will enable the differentiation of bound gas from disk winds, allowing for the derivation of physical parameters such as density, temperature, and ionization fraction. Observations of circumstellar disks around young stellar objects of various ages will help trace the evolution of disks from protostellar stages (around 100,000 years old) to more evolved phases (up to 10 million years old). This will shed light on how disks dissipate and how planetary systems form and evolve. ANDES will examine the different mechanisms contributing to gas dispersal in the inner disk, such as magnetospheric accretion, jets, and disk winds. High-resolution data will help distinguish these mechanisms and quantify their impact on disk evolution. The data obtained from ANDES will complement observations from mid-infrared instruments like JWST/MIRI and ELT/METIS, providing a comprehensive understanding of protoplanetary disk dynamics and their role in planet formation.

A detailed description of the science objectives in the field of exoplanets and protoplanetary disk is provided in the white paper by Palle at al.[4]

2.2 Stars and Stellar Populations

The study of stars and stellar populations is fundamental to understanding the formation and evolution of galaxies. Stars are the primary building blocks of galaxies and serve as the key drivers of chemical enrichment and energy distribution within these systems. By investigating the properties of stars in various evolutionary stages and environments, astronomers can reconstruct the history of star formation and the processes that govern stellar evolution. This knowledge is crucial for interpreting observations of distant galaxies and for refining theoretical models of galaxy formation and evolution. Key scientific objectives for ANDES in the study of stars and stellar populations are the following.

First Stars. The first stars, or Population III (Pop III) stars, are believed to have formed from metal-free gas at redshifts greater than 15-30. These stars played a crucial role in ending the cosmic Dark Ages by producing the first ionizing photons, supernovae, metals, and stellar-mass black holes. Despite their significance, Pop III stars have not been directly observed. ANDES aims to reveal the nature and end states of these stars by searching for

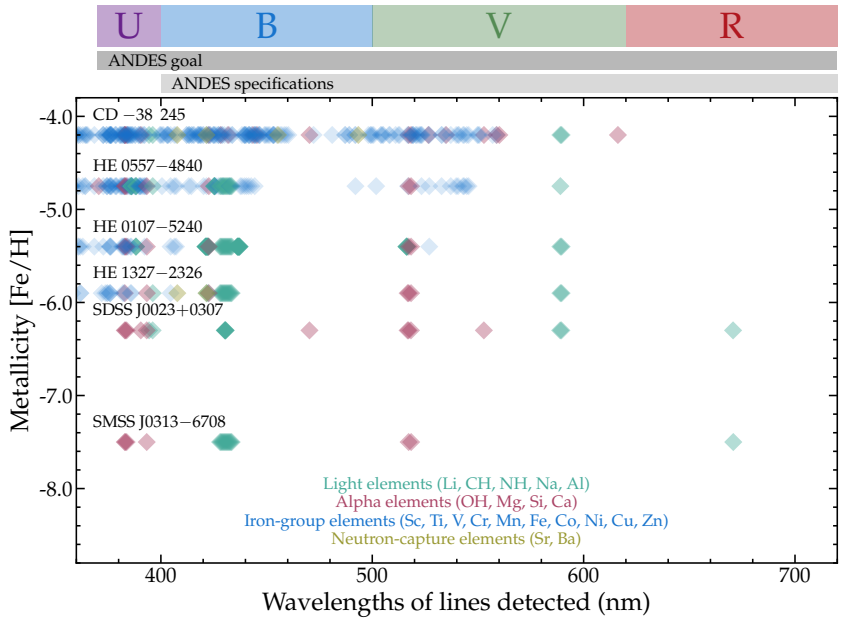

Figure 2. Wavelengths of absorption lines detected in the optical spectra of six stars known at present with [Fe/H] < -4. Each point represents one line in one star, and different elements are marked by different colors. The design of ANDES will enable the detection of the vast majority of these lines, covering all major nucleosynthesis groups, in many more stars that retain the fossil records of metals produced by the first stars. Figure from Roederer et al.[5]

long-lived, low-mass metal-free Pop III stars. The high spectral resolution (R $\sim$ 100,000) of ANDES is critical for detecting the faint spectral lines of hydrogen without contamination from metal lines (see, e.g., Fig. 2). By collecting spectra of candidate metal-free stars with [Fe/H] < -4, ANDES can provide stronger constraints on the characteristic mass and low-mass end of the Pop III initial mass function (IMF).

Stellar Populations in the Galactic Bulge. Understanding the age distribution of stars in the Galactic bulge is essential for deciphering the formation and evolution processes of this region. Observational evidence on this topic is conflicting, with some studies suggesting the bulge is almost entirely old, while others report a significant fraction of young and intermediate-age stars. ANDES, with its large collecting area of the ELT, will obtain high-resolution spectra of turnoff and subgiant stars in the bulge, even without gravitational microlensing magnification. These spectra will enable the determination of parameters, metallicities, and detailed chemical abundances, allowing for stellar age inference with about 25% precision (Fig. 3). The broad wavelength coverage (0.40 to 1.80 μm) and high signal-to-noise ratios provided by ANDES are crucial for identifying and analyzing the numerous spectral lines necessary for these determinations. These data will help map the age distribution across the bulge and provide novel constraints on its formation and connections to other stellar populations.

Stellar Populations in Dwarf Galaxies. The Local Group's dwarf galaxies offer unique insights into hierarchical mass assembly. These galaxies, spanning a wide range of stellar masses and chemical compositions, are prime targets for studying the imprints of the first stars and the earliest nucleosynthesis events. ANDES will enable high-resolution and high-signal-to-noise optical spectroscopy of stars in these galaxies, which are often too faint for current telescopes. This capability will allow for detailed chemical compositions to be derived, providing insights into the progenitors of supernovae, the production of heavy elements, and the origins of extreme carbon enhancement observed in many metal-poor stars. The adaptive optics integration with ANDES will enhance its capability to obtain high-quality spectra of these faint stars, making it possible to study their detailed compositions and evolutionary histories.

In summary, the capabilities of ANDES are integral to advancing the study of stellar populations. By providing high-resolution spectra, broad wavelength coverage, and the ability to observe faint and distant stars,

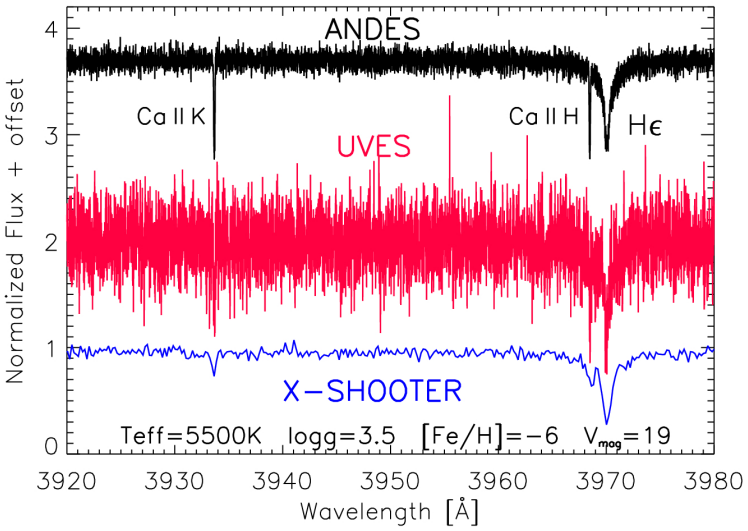

Figure 3. A simulated 1-hour spectrum of a subgiant second-generation star with a total metallicity of 10^{-6} times the Solar metallicity in the U channel around Ca II H & K lines. Random noise has been added to simulate the S/N for ANDES (black), UVES (red), and X-SHOOTER (blue). Figure from Roederer et al.[5]

ANDES will significantly enhance our understanding of the formation and evolution of the first stars, the Galactic bulge, and dwarf galaxies in the Local Group. These studies will provide critical insights into the processes governing stellar evolution and the formation of galaxies.

A detailed description of the science objectives for stars and stellar populations is provided in the white paper by Roederer et al.[5]

2.3 Galaxy Formation and evolution and the intergalactic medium

The study of the reionisation epoch (EoR) is crucial for understanding the formation and evolution of the universe's first structures. This epoch marks the transition from a neutral to an ionized intergalactic medium (IGM) to the emergence of the first luminous sources. Absorption spectroscopy of high-redshift quasars and gamma-ray bursts (GRBs) provides a direct probe into the conditions of the IGM during this transformative period. ANDES will be able to addresse several important science goals detailed below.

Characterising the Epoch of Reionisation. The high spectral resolution (R $\sim$ 100,000) of ANDES will enable precise measurements of the Lyman-α and Lyman-β forests in the spectra of $z \geq 6$ quasars and GRBs. By resolving these lines, ANDES will map the distribution of neutral and ionised hydrogen in the IGM, allowing us to track the progression of reionisation (Fig. 4). Detailed studies of these forests will reveal the size and distribution of ionised bubbles and neutral patches, shedding light on the sources driving reionisation, such as the first stars, galaxies and active galactic nuclei (AGNs). The unprecedented sensitivity of ANDES, owing to the ELT's large collecting area, will allow us to observe fainter quasars and GRBs, increasing the number of targets and providing a statistically significant sample strengthening constraints on the size and distribution of ionised and neutral regions, offering a more nuanced picture of how reionisation progressed spatially across the universe.

Chemical Enrichment of the Early Universe. Above redshift z $\sim$ 5.5, the Lyman forest becomes less informative due to complete absorption of the quasar flux. However, ANDES's ability to detect metal absorption lines in the near-IR spectrum will allow studies of the the IGM physical and chemical properties even when hydrogen lines are saturated. ANDES's broad wavelength coverage (0.4-1.8 μm, with a goal of 0.35-2.4 μm) will allow simultaneous observation of multiple absorption lines from various elements such as carbon, oxygen, silicon and iron within the epoch of Reionization. In particular, the transition OI at 1302 A is a tracer of neutral gas and can provide a complementary probe to the Lyman-series lines to study the ionization state of the IGM.

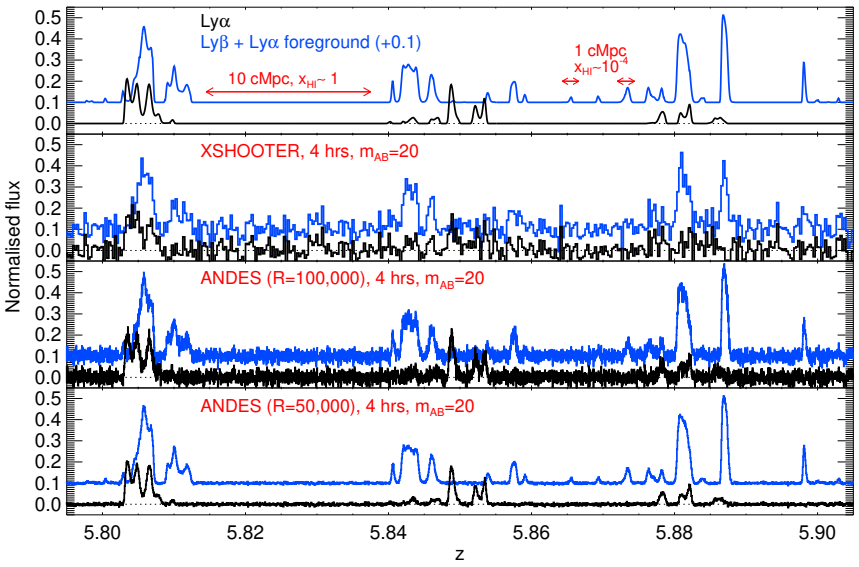

Figure 4. The upper panel shows a segment of the Lyman-α (black curve) and coeval Lyman-β (blue curve) forests in the spectrum of a z = 6.1 quasar, drawn from a cosmological hydrodynamical simulation coupled with radiative transfer. Note that the Lyman-β forest flux has been offset by +0.1 for presentation purposes, and it also includes foreground Lyman-α forest absorption. The lower three panels show simulated observations with an exposure time of 4 hours assuming a magnitude $m_{AB} = 20$ for the target quasar, obtained with (from top to bottom): VLT-XSHOOTER at R$\sim$ 10,900) with S/N$\sim$12, ELT-ANDES for the baseline resolution of R = 100,000, reaching S/N$\sim$80 and for the lower resolution mode with R = 50,000 with S/N$\sim$110. All signal-to-noise ratios are per 10 km/s spectral element. Figure from D'Odorico at al.[6]

Additionally, the measurement of the detailed chemical abundances in dense neutral environments will be crucial to detect the signatures of the enrichment by the first generation of stars (Fig. 5). In this respect, ANDES will allow for the first time to measure critical trace elements such as Zinc (Fig. 5). By detecting and analyzing these metal lines, ANDES will provide insights into the production and distribution of heavy elements in the early universe, helping us understand the contribution of the first supernovae and the initial stages of galaxy formation.

Understanding the Relationship Between Galaxies and the IGM. ANDES will also facilitate the study of the relationship between galaxies and the IGM by correlating absorption features with galaxies detected in emission through other instruments like JWST. This multi-wavelength approach will help us understand how galaxies influenced their surroundings and contributed to the reionisation process. By combining absorption and emission data, ANDES will provide a comprehensive view of the interactions between galaxies and the IGM, offering insights into the feedback mechanisms that regulated star formation and galaxy growth. The fine spectral resolution of ANDES will enable precise measurements of the thermal broadening of absorption lines, allowing to infer the temperature of the IGM during the reionisation epoch. Understanding the thermal state of the IGM is essential for constraining the sources of heating, such as UV radiation from early galaxies and quasars. The thermal history provides critical information about the energy budget of the universe and the efficiency of ionising photon production. ANDES's ability to resolve these thermal features will help refine models of IGM heating and cooling processes.

Extragalactic transients. Extragalactic transients, such as gamma-ray bursts (GRBs), superluminous supernovae (SLSNe), and novae, provide crucial insights into the physical and chemical properties of their host galaxies. These short-lived events are often faint, posing significant observational challenges that ANDES aims to overcome with its unprecedented sensitivity and near-infrared capabilities. GRBs, associated with massive star explosions, serve as cosmic beacons to study the interstellar medium (ISM) of distant galaxies. SLSNe, being 10 to 100 times more luminous than typical supernovae, can be observed at high redshifts, shedding light on the

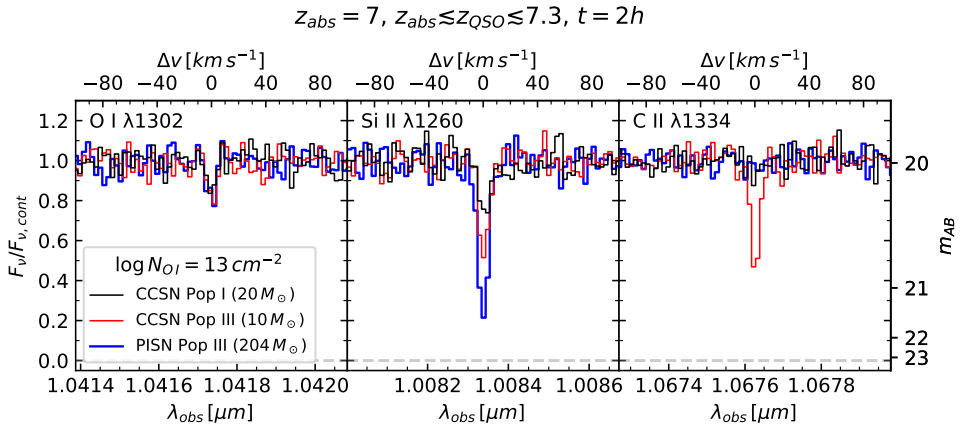

Figure 5. Simulated ANDES spectrum of a metal absorption system at $z = 7.0$, with N(O I) $= 10^{13} cm^{-2}$ along the line of sight to a background $m_{AB} = 20$ quasar observed for 2 hours. The panels display zoomed-in regions around the OI λ1302, SiII λ1260 and CII λ1334 absorption features in three different scenarios enriched by the ejecta from: the core collapse supernova (CCSN) of a $Z = 1/3 Z_\odot$, $m_\star = 20\,M_\odot$ star (black line), the Pop III CCSN of a $m_\star = 10\,M_\odot$ star (red line) and the Pop III PISN from a $m_\star = 204\,M_\odot$ star (blue line). The three scenarios can be clearly distinguished from the ANDES spectrum. Figure from D'Odorico at al.[6]

properties of low-metallicity host galaxies. The exact mechanisms behind these explosions remain debated, with potential links to very massive stars or Population III stars. Classical novae involve thermonuclear explosions on white dwarfs and provide insights into the synthesis of heavy elements like lithium. ANDES's high resolution and wide spectral coverage will enable detailed studies of these transients, enhancing our understanding of the early universe and the lifecycle of galaxies. Rapid response modes will be particularly beneficial for capturing the transient phases of GRBs, ensuring timely and detailed observations.

In summary, the capabilities of ANDES will allow for unprecedented studies of the reionisation epoch, providing detailed maps of the ionisation state, chemical enrichment, and thermal history of the early universe. These studies are essential for understanding the formation and evolution of the first cosmic structures and the processes that shaped the universe as we see it today.

A detailed description of the science objectives for galaxy formation and evolution, and the intergalactic medium is provided in the white paper by D'Odorico at al.[6]

2.4 Cosmology and Fundamental Physics

Spectroscopy has historically been a catalyst for significant advancements in fundamental physics. In the 21st century, ANDES at ESO's ELT is poised to continue this tradition, offering unprecedented opportunities to probe the fundamental aspects of the universe. By leveraging high-resolution spectroscopy, ANDES aims to address critical questions in cosmology and fundamental physics. Here we outline the primary scientific goals and the key capabilities of ANDES that will enable these investigations.

Big Bang Nucleosynthesis (BBN). Big Bang Nucleosynthesis provides a critical probe of the early universe by measuring the primordial abundances of light elements such as deuterium (D), helium-3 (^{3}He), helium-4 (^{4}He), and lithium-7 (^{7}Li). These abundances are sensitive to the baryon density, the expansion rate, and the particle content of the universe, thus offering insights into potential deviations from the Standard Model of particle physics and cosmology. ANDES's high spectral resolution (R∼100,000) will allow for the precise measurement of the primordial ratios of D/H, ^{3}He/^{4}He, and ^{7}Li/H in quasar absorption line systems. The large collecting area of the ELT will facilitate observations of faint, distant objects necessary for accurate abundance measurements, testing the consistency of the cosmological model and the Standard Model. By combining measurements of multiple primordial elements with theoretical BBN calculations, ANDES aims to

uncover any deviations from the Standard Model. The wide wavelength coverage (0.35–2.4 μm) is crucial for capturing the necessary spectral lines across various redshifts, providing a comprehensive test for new physics.

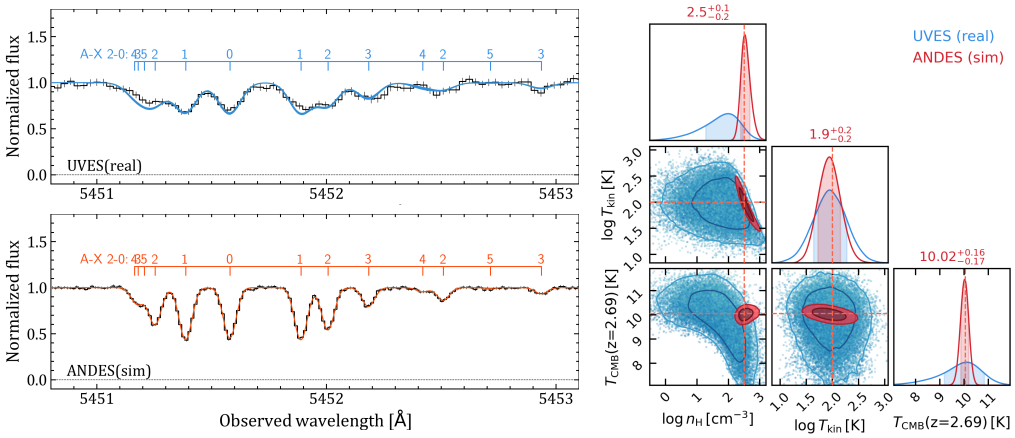

Figure 6. Left: An example of CO absorption band observed at z = 2.69 towards the quasar J1237+0647 with VLT/UVES (R = 50000, S/N∼40/pixel), and as expected with ANDES with R = 100000, S/N∼100 pixel/1. The numbered tick lines indicate the different rotational levels that compose the band. Right: Simultaneous constraints on CMB temperature, density and kinetic temperature using profile fitting of CO lines coupled with excitation model for CO rotational levels. The blue and red colours represent the constraints obtained using existing UVES spectrum and a forecast for ANDES, respectively. Figure from Martins at al.[7]

Evolution of the Cosmic Microwave Background Temperature (T_{CMB}). The evolution of the CMB temperature as a function of redshift is a fundamental prediction of the standard cosmological model. Deviations from the expected $T_{CMB}(z) = T_{CMB}(0)(1 + z)$ relationship could signal new physics, such as violations of the Einstein Equivalence Principle or variations in the fine-structure constant. ANDES will leverage its high sensitivity and precision wavelength calibration to measure the CMB temperature at different redshifts with high accuracy. This capability is essential for testing the adiabatic expansion and photon conservation predictions of the standard model. By detecting or placing stringent limits on deviations from the expected T_{CMB} evolution, ANDES will explore potential new physical phenomena. The instrument's ability to achieve precise measurements of the thermal state of the IGM will be pivotal in identifying any such deviations (Fig. 6).

Tests of the Universality of Physical Laws. One of the flagship science cases for ANDES involves testing the constancy of fundamental physical constants, such as the fine-structure constant (α) and the proton-to-electron mass ratio (μ). Any variation in these constants over cosmic time could indicate new forces or fields not accounted for in the Standard Model. Utilizing its extremely high spectral resolution, ANDES will conduct precise measurements of α and μ in various environments and redshifts, examining their constancy over time. This will involve comparing the relative frequencies of multiple transitions in quasar spectra, enabled by the instrument's broad wavelength range. By investigating potential deviations from the universality of physical laws, ANDES will search for new interactions or particles. The ability to measure fundamental constants in different regions of space-time will help identify any composition-dependent forces, providing insights into the underlying physics.

Real-Time Mapping of the Expansion History (Redshift Drift) ANDES will perform real-time measurements of the redshift drift, providing a direct, model-independent probe of the universe's expansion history. This method, also known as the Sandage-Loeb test, measures the change in redshift of distant objects over time, offering a unique perspective on the dynamics of cosmic expansion. ANDES will utilize its long-term stability to detect the subtle changes in redshift over decades, providing a direct and model-independent measurement of the cosmic expansion history. This will involve monitoring the redshifts of Lyα forest and other absorption lines in quasar spectra. By combining redshift drift data with other cosmological observations, ANDES will constrain or refine models of dark energy and the overall cosmological paradigm. The instrument's high collecting power

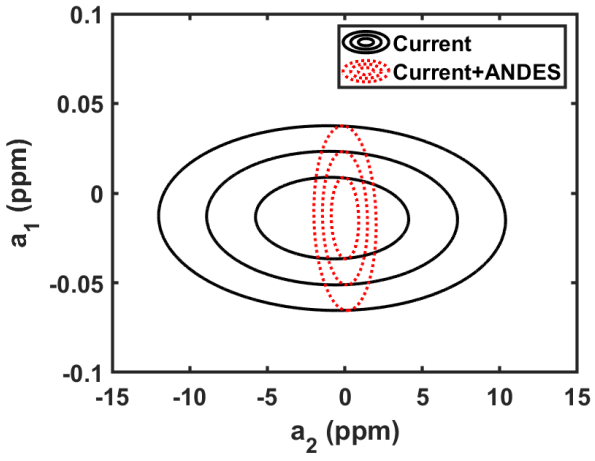

Figure 7. Model-independent constraints on the variation of the fine structure constant α parameterized as $\Delta\alpha/\alpha = a_1 * y + (1/2) * a_2 * y^2$ with $y = z/(1+z)$. a_1 is mainly constrained by laboratory experiments, while a_2 can only be constrained through astrophysics. Black contours show current constraints, while the red ones include a simulated dataset of ANDES measurements from 15 absorbers, with all other data unchanged. Figure from Martins at al.[7]

is essential for gathering sufficient photons from distant, faint quasars, achieving the precision required for this groundbreaking measurement.

Summarizing, ANDES at the ELT will significantly advance our understanding of cosmology and fundamental physics. By integrating high spectral resolution, broad wavelength coverage, and a large collecting area into its design, ANDES will enable detailed studies of the early universe, the evolution of fundamental constants, and the real-time expansion history of the cosmos. These capabilities position ANDES as a critical tool for exploring new physics and refining our cosmological models in the coming decades. A detailed description of the science objectives for cosmology and fundamental physics is provided in the white paper by Martins at al.[7]

2.5 Science Priorities

Only a very expensive instrument would fulfil the requirements associated with the top priority science cases identified within each science area. Therefore, an overall science prioritization was performed by the core SAT during Phase A to drive the corresponding process of instrument design and to establish a trade-off between cost and scientific priorities. The following criteria were identified:

- Scientific impact: transformational versus incremental.
- Feasibility.
- Competitiveness.

Also, if the TLR's of the top priority science case were enabling other science cases, the latter were not considered any further in the subsequent prioritization, as considered accomplished together with the top priority science case. The top science priorities are listed below and were used to define the technical specifications. We remark that these are not absolute science priorities, but science priorities identified with the aim of driving the instrument design.

1. **Exoplanet atmospheres in transmission.** The TLRs for the study of exoplanet atmospheres (mainly $R \sim 100,000$, 0.5-1.8 μm spectral range and wavelength calibration accuracy of 1 m/s) also enable the following science cases: reionization of the universe, the characterization of cool stars, the detection and investigation of near pristine gas, the study of extragalactic transients.

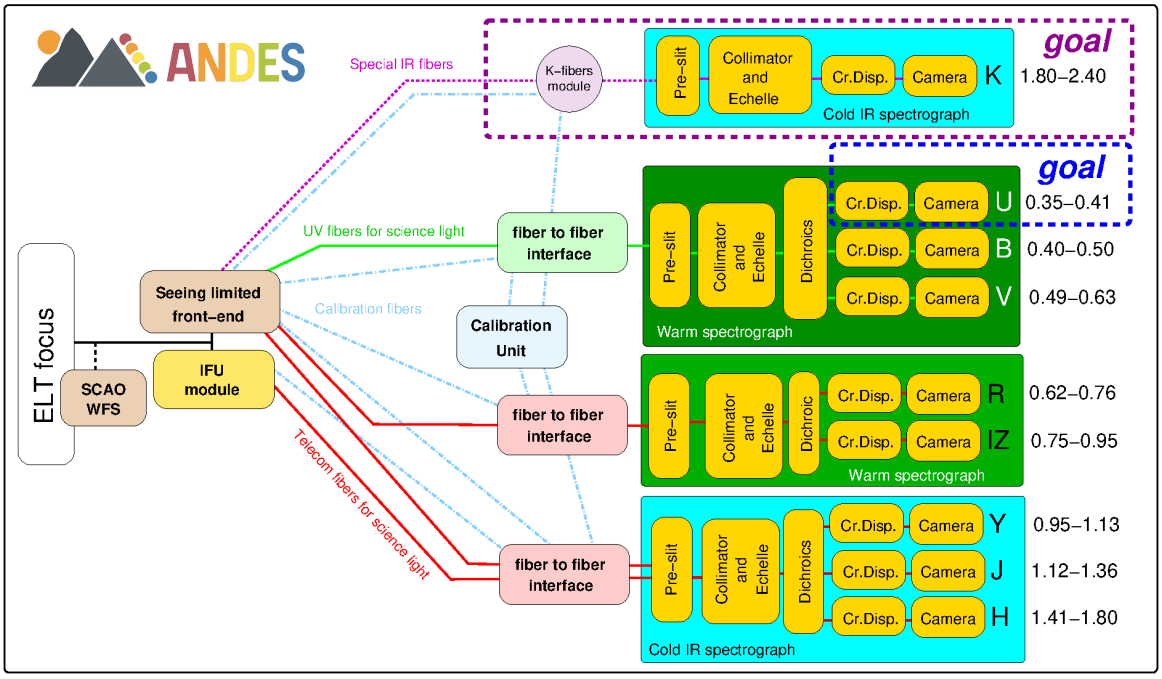

Figure 8. ANDES architectural design, outlining the instrument subsystems: Front End (seeing-limited and AO assisted with SCAO unit), Fibre Link, Calibration Unit, [U]BV, RIZ, YJH and K (cold spectrographs). Andes Logo by Alexis Lavail (Uppsala).

2. **Variation of the Fundamental Constants of Physics,** requiring an extension to 0.37 μm and automatically enabling to investigate: the cosmic variation of the CMB temperature, the determination of the deuterium abundance, the investigation and characterization of primitive stars. At $\lambda < 0.40$mm the throughput of the ELT is expected to be low as a consequence of the planned coating. However, even in the range 0.37-0.40 μm the system is expected to be competitive with ESPRESSO.

3. **Detection of exoplanet atmospheres in reflection,** requiring an Adaptive Optics (SCAO) system and an Integral Field Unit. These additional TLRs also automatically enable the following cases: Planet formation in protoplanetary disks, Characterization of stellar atmospheres, Search of low mass Black Holes.

4. **Sandage test.** Its additional TLR of a stability of 1 cm/s, enables also: radial velocity searches and mass determinations of Earth-like exoplanets.

This prioritization and the corresponding top level requirements finally resulted in the Technical Specifications whice were officially issued by ESO prior to the beginning of Phase B1 and which were used to drive the baseline design.

3. INSTRUMENT CONCEPT

The ANDES baseline design is that of a modular fibre-fed cross dispersed echelle spectrograph which has three ultra-stable spectrometers, [U]BV, RIZ and YJH, providing a simultaneous spectral range of 0.4-1.8 μm at a resolution of ~100,000. The goal is to extend the wavelength range to 0.35-2.4 μm with the addition of an U arm to the BV spectrograph and a separate K spectrograph. The instrument can operate in seeing limited as well as in a SCAO-assisted mode. In seeing-limited mode it allows for simultaneous sky and/or calibration measurements. In SCAO mode it uses a small IFU with at least two selectable spaxel scales (only in the YJH spectrometer, also in the RIZ spectrometer as a goal). The seeing-Limited mode will be quite unique among the ELT suite of instruments and will allow observations even in bad atmospheric conditions and/or with poor

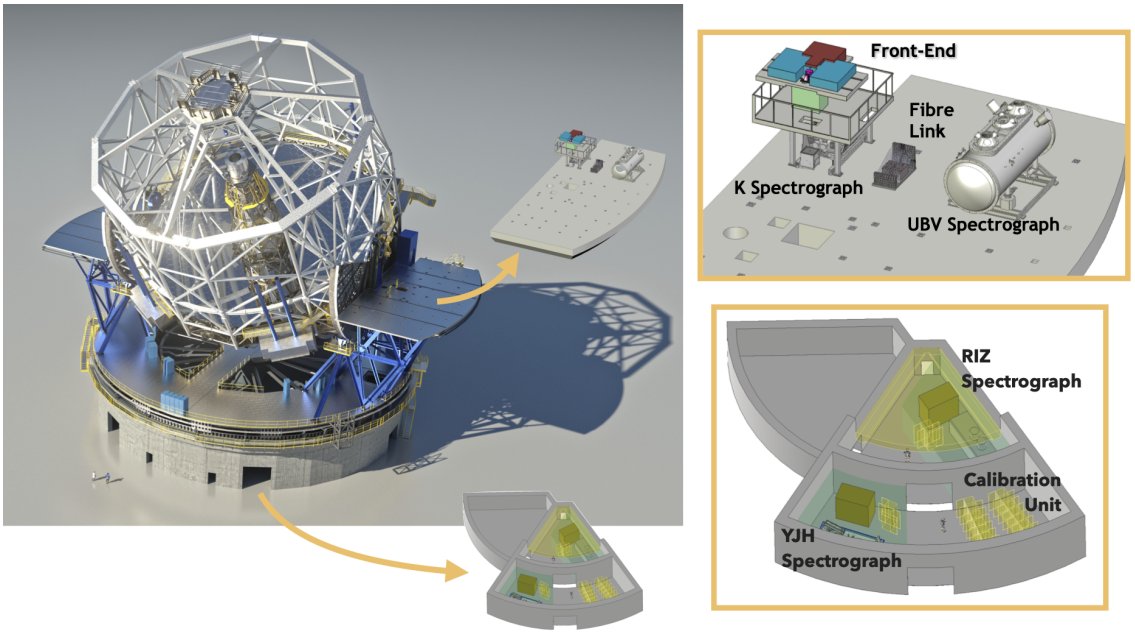

Figure 9. Overall and detailed views of ANDES Nasmyth and Coudé parts in the case the instrument is not entirely placed on the Nasmyth platform.

phasing of the ELT mirrors. It will also require simpler telescope operations. The expected limiting magnitude for seeing limited observations is $m_{AB} = 20$ in 1 hr with SNR=10 per resolution element. Simulations can be performed with the live ETC maintained by INAF-Arcetri at andes.inaf.it. This ETC can compute the limiting magnitude achievable at a given wavelength, for a given exposure time and at a given signal to noise ratio or it can compute the signal to noise ratio achievable at a given wavelength, in a given exposure time and at a given magnitude. With these observing modes and the expected performances, the proposed baseline design can fulfil the requirements of the 3 top science cases discussed in Sec. 3, with the goal of fulfilling also the 4th one. The proposed baseline of the system is shown in Fig. 8, which provides a schematic view of the functional architecture and illustrates the modularity level chosen for the instrument. The major subsystems composing the instrument are presented as boxes, connected by fibers or fiber bundles that serves for delivering the light from the ELT focus and from the Calibration Unit(s) to the various Spectrographs that are located in different parts of the Telescope Infrastructure, the Nasmyth Platform and the Coudé room. If enough volume and mass are available, the instrument can be placed entirely on the Nasmyth platform. Alternatively, the [U]BV and K modules can be placed on the Nasmyth platform while the other modules will sit in the Coudé Room (Figure 9). The split in wavelengths over the modules is influenced, among all other parameters by the optical transparency of the different types of fibres available on the market. Therefore, the different modules can be positioned at different maximum distances from the telescope focal plane. The proposed configuration foresees that [U]BV is in the Nasmyth platform while the RIZ and YJH spectrometers are in the Coudé Room with the corresponding Fibre-to-Fibre interfaces and dedicated Calibration Units (that, for simplicity, is represented as one single box in Figure 8).

During operations, the light from the telescope pre-focal station reaches the Front-End, a structure that is positioned on the Nasmyth platform and includes four independently insertable modules: two seeing limited arms, one SCAO arm and one IFU arm.

Depending on the chosen operational mode, the instrument is capable of inserting the different modules and delivering the light to specific modules. Regardless of the specific observing mode, the Front End splits the light from the telescope via dichroics, provides proper optical correction and feeds the fibre bundles with the light divided into different spectral channels according to the wavelength bands reported in the picture and part of

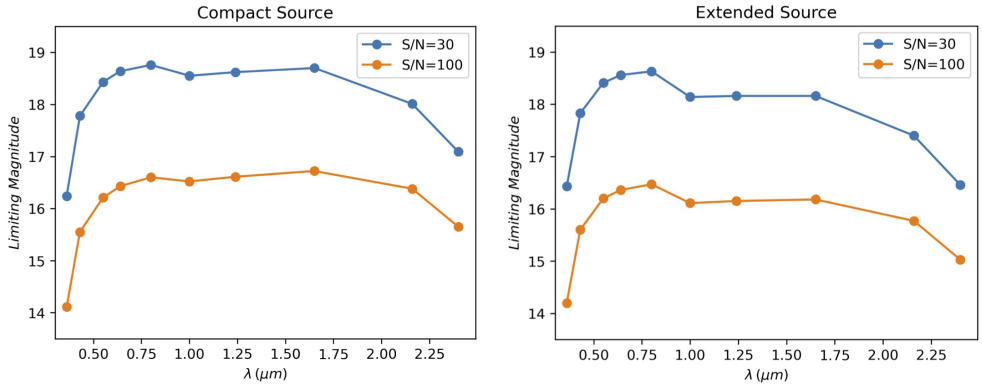

Figure 10. ANDES limiting magnitudes obtained from the ETC for different S/N ratios (30 – top and 100 – bottom), compact and extended sources (left and right). Observations are in seeing-limited mode with R = 100,000 a total exposure time of 1800s.

the TRS. The Fiber-Link subsystem is in charge of transporting the light to the spectrographs (also down to the Coudé room, Fig 9) and forming a series of parallel entrance slits, each consisting of an array of micro-lenses optically coupled to a fiber bundle. The fibre bundles are divided into two segments and have two different routings. The first segment connects the Front End to the Fibre-to-Fibre interface boxes, while the second segment connects the Fibre-to-Fibre interface boxes to the spectrographs. The two segments carrying the IFU light are directly connected, to maximize throughput; while the segments carrying the light from the seeing-limited apertures are coupled via a double scrambler optical system, to optimize precision and accuracy. The Fibre-to-Fibre boxes lie close to the spectrometers, i.e., the BV interface is on the Nasmyth platform while the infrared (RIZ and YJH) interfaces are in the Coudé room. All spectrometer modules have a fixed configuration, i.e., no moving parts and provide proper spectral resolution and sampling in the requested wavelength range. The calibration unit includes proper calibration sources for feeding the Front-End and the Fibre-to-Fibre interfaces (part of the FL) through a suitable routing of fibres. Several analyses have been performed in order to define the best trade-off for the wavelength splitting and in particular, much effort has been dedicated to push the spectrographs as much as possible toward the goal ranges, including the U-Band in the BV spectrograph and an additional subsystem (fibres and spectrograph) for the K-band to be located on the Nasmyth platform.

Summarizing, the main subsystem of ANDES are as follows (see also Figure 8):

- Front End (FE) which transfers the light from the ELT Nasmith focus to the rest of the instrument, with 4 separated modules: two seeing limited and two for the IFU and SCAO modules.
- Fibre Link (FL) which couples the light coming from the Front End fibre bundles into the fibre bundles that feed the spectrographs.
- Single Conjugated Adaptive Optics (SCAO) aimed to provide the adaptive optics correction to the IFU feeding the YJH spectrograph.
- Calibration Unit (CU) whose aim is to deliver calibration light for the ANDES spectrographs on demand and is connected via fibres to the Front End through the Fibre Links.

and the Spectrographs:

- UV-optical Spectrograph ([U]BV). The [U]BV module has 3 cameras: V, B and U (goal) with one scientific detector each. The U arm/camera is an option under study to extend the wavelength coverage toward the blue.